

Photoetched Regenerator for Use in a High Frequency Pulse Tube

W.F. Superczynski, G.F. Green

Chesapeake Cryogenics, Inc.
Arnold, MD 21012

ABSTRACT

To produce refrigeration at 20 K in a single stage regenerative cryocooler requires a combination of materials that possess high heat capacity within its operational temperature range. This has typically been accomplished using woven screens made of stainless steel or phosphorous-bronze operating in the 300 K to 50 K range followed by a packed bed of spheres made of lead or other rare earth material. However, screens and particularly spheres produce high pressure losses within the regenerator. In a pulse tube operating at higher frequencies (40 to 60 Hz) where the pressure ratio is on the order of 1.3, the pressure loss becomes a more significant factor and prevents achieving 20 K. Therefore, Chesapeake Cryogenics, Inc. (CCI) is investigating the use of a gap-type regenerator employing both conventional materials and rare earths. The flow channels are created by a photochemical etching process to generate slots in disks. The disks are then stacked in the regenerator aligning the slots to produce parallel channels in the axial direction. The photochemical machining process may provide sufficient dimensional tolerances and repeatability resulting in uniform channels with heat transfer surface area approaching that of screens and spheres. Furthermore, this etching process can be applied to rare earth materials making the disks suitable for use at temperatures below 50 K. CCI has performed preliminary tests to determine the pressure loss under steady flow conditions, thermal conduction, and cryocooler performance using photoetched disks made of phosphorous-bronze and stainless steel to determine their suitability as replacements for screens and spheres. Results of these tests and a description of the flow channel geometry are presented.

INTRODUCTION

Regenerator matrices operating from 300 K to 20 K are typically composed of woven phosphorous-bronze or stainless steel screens followed by lead spheres in the cold portion. It has been shown that parallel plates will permit a smaller pressure loss penalty per unit of heat transfer thereby reducing the PV work loss term in the expansion volume.¹ However, past attempts to take advantage of this concept by implementing a parallel plate design in cryogenic regenerators have not been successful. Therefore, we are taking another approach, not relying on the empirical data available from sources such as Kays and London. In this effort, the heat transfer correlations will be modified in the modeling program to predict measured cooler performance. After the model has been shown to accurately predict measured performance subsequent to modifying the heat transfer correlations, the new correlations will be used to model and optimize the regenerator design to meet the performance design point of 2 W at 20 K. Attaining refrigeration at 20 K will also require material that



Figure 1. Schematic of channel section shape after chemical etching.

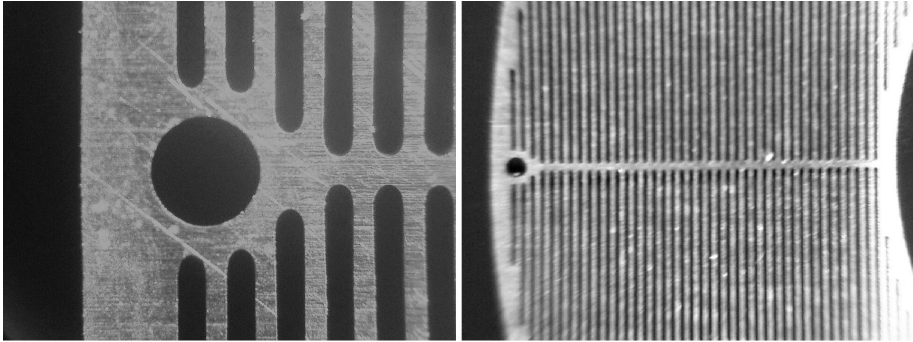


Figure 2. Photomicrographs ($\sim 50\times$ and $13\times$) of etched disks created in phosphorous bronze material using PCM.

possess high enough heat capacity to prevent large temperature oscillations at the cold end. Therefore, we will look at the feasibility of producing photoetched regenerators composed of rare earth materials. It will also be necessary to determine the tolerance limits.

REGENERATOR MATRIX ASSEMBLY

Photochemical machining (PCM) is an economical method of selectively removing material from sheet stock to produce precision parts. The process involves printing a phototool which is a photo positive of the part to be fabricated. The phototool may contain many copies of the part enabling simultaneous machining of many pieces. A photoresist is then adhered to both sides of the metal sheet from which the parts are to be machined. Using the phototool, the photoresist is selectively exposed to ultra violet light which polymerizes the resist. The unexposed resist is then washed from the sheet and the material is sprayed with an acid etchant, dissolving the exposed metal. During this process, the part is held to the sheet with a small tab which is broken after the machining process has completed to remove the part. The parts are then washed in an alkaline solution to stop the etching process and remove the remaining photoresist.

The photo etching process has dimensional limitations because the etchant removes metal both laterally and through the thickness of the sheet. This results in curvature of the sides of the etched surface as shown in Fig. 1. For thru features, the minimum dimensions are related to the material thickness. The minimum size of a feature is approximately 1.2 times the material thickness with a minimum practical size of $89\ \mu\text{m}$ (0.0035in) for a slot and $127\ \mu\text{m}$ (0.005in) for a hole. This limited the hydraulic diameter attainable with this etching process to approximately $178\ \mu\text{m}$ (0.007in) for a slotted disk. It also necessitates the use of sheet stock no thicker than $76\ \mu\text{m}$ (0.003in). The disks were pinned to align the slots of adjacent disks, effectively creating axial ducts along the regenerator length. The pin is a stainless steel tube $381\ \mu\text{m}$ (0.015in) diameter with a $102\ \mu\text{m}$ (0.004in) wall thickness. Figure 2 is a photomicrograph of a phosphorous bronze disk, and Fig. 3 is the design drawing from which these parts were produced. The inside and outside diameter were dictated by the cryocooler dimensions and configuration into which the disks will replace the screen geometry in order to obtain performance data.

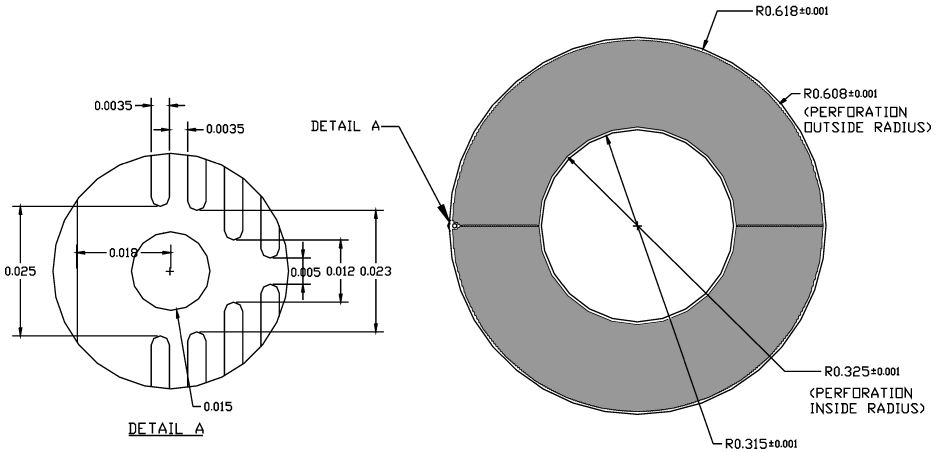


Figure 3. First order design drawing of etched disk regenerator for pulse tube regenerator.

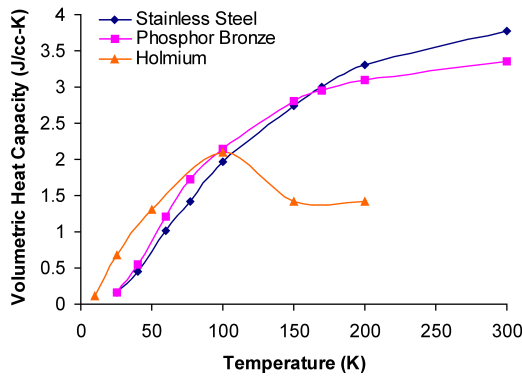


Figure 4. Temperature dependency of volumetric specific heat for materials used in regenerator design.

The possibility of applying this same etching process to rare earth metals was also investigated. Because of the photochemical machining processes and the fabrication techniques used to produce the parallel channels, the material must be available in flat sheet. In order to help attain the goal of 20 K, holmium was selected as the material with the most favorable volumetric heat capacity characteristics. Figure 4 shows the advantage of using holmium rather than stainless or phosphorous bronze based on its higher volumetric heat capacity at temperatures below approximately 100 K. A small sample of holmium was etched to demonstrate the feasibility of utilizing this same fabrication technique. Etching qualities of holmium are very similar to that of phosphorous bronze, and attaining the current dimensional limitations was shown feasible. Figure 5 is a photomicrograph of the holmium sample fabricated using PCM. Etched disks of holmium were not fabricated with dimensions shown in Fig. 3 during this phase of the program, because material expense was cost prohibitive.

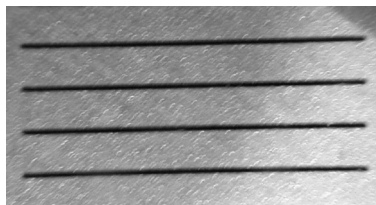


Figure 5. Photomicrograph of slots etched in Holmium sheet.

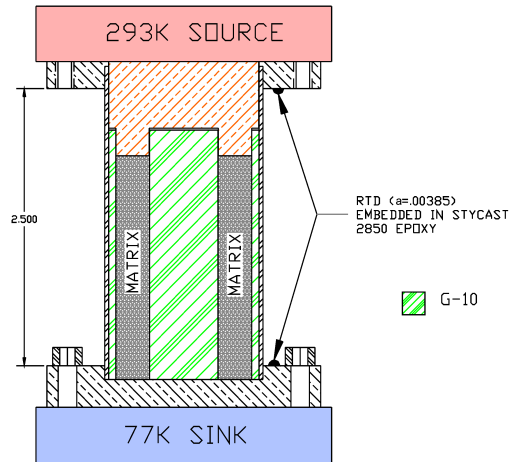


Figure 6. Schematic of conduction test apparatus used to determine degradation factor.

Cryocooler performance improvements using high heat capacity materials at low temperatures are to be determined using modeling software assuming the same heat transfer and pressure drop correlations apply using disks fabricated from holmium with identical hydraulic diameter to that of the phosphorous bronze.

ETCHED DISK LOSSES

Tests were conducted in an attempt to quantify the conduction and pressure loss mechanisms occurring in the regenerator matrix composed of etched disks. Identifying the magnitude of these losses is considered essential to accurate modeling of the regenerator performance enabling design for 2 watts at 20 K.

Conduction

Heat conduction tests were conducted on both stainless steel and phosphorous-bronze etched disks stacks. Figure 6 is a drawing of the conduction apparatus. The cold end is in contact with a liquid nitrogen bath to maintain a temperature of approximately 77 K. The warm end is maintained at a temperature of 293 K by modulating power to a cartridge heater. The G-10 sleeves were used to align the disk stack and prevent the motion of helium along the inside and outside diameter surfaces of the stack. The heat conducted through the apparatus with no matrix present was measured first. This was used to establish a baseline and allowed the net heat conducted through a matrix stack to be determined by reducing the total measured heat conducted by the baseline value. Measuring the steady state net conduction of heat (Q_n) allowed the conduction degradation factor (δ) to be determined from Eq. (1):

$$\delta = \frac{Q_n L}{k_{ave} A (1 - \alpha) \Delta T} \quad (1)$$

In this equation, L is the total length of the etched disk stack, k_{ave} is the average conductivity, A is the regenerator cross sectional area, α is the porosity of the matrix, and ΔT is the temperature difference between the warm and cold end, which was maintained constant at 216 K. Table 1 shows the conduction degradation factor that was measured for Ph-Bronze and stainless steel etched disks. This degradation factor is an optional input parameter in the regenerator modeling program which helps to improve the solution accuracy. The product of the degradation factor and thermal conductivity gives an indication that the total heat flow through the Ph-Bronze matrix will be about 41% higher. However, if we consider the total heat flow due to conduction through the regenerator housing and pulse tube walls, the effect of the material choice will increase the total conduction loss

Table 1. Results of conduction testing of etched disks made from different materials.

Material	k_{ave} [W/cm-K]	δ [dimensionless]	$k_{ave}\delta$ [W/cm-K]
Stainless Steel	0.123	0.077	0.0095
Phosphorous-Bronze	0.480	0.028	0.0134

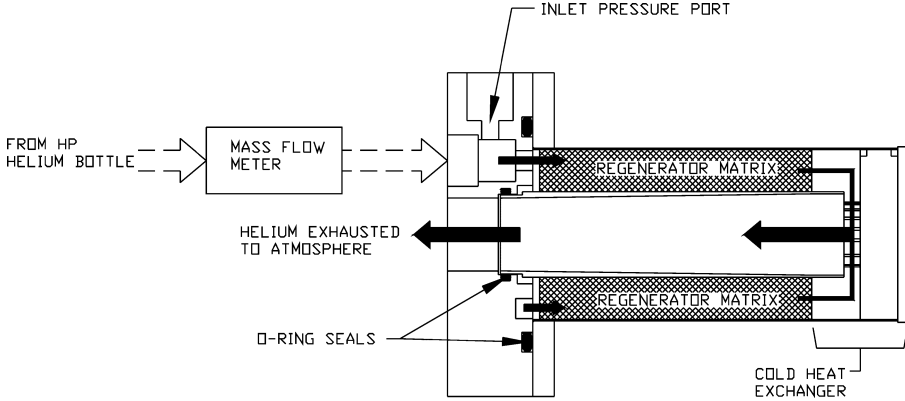


Figure 7. Schematic of test set-up used to determine friction factor under steady flow conditions.

by 18%. It is suspected that the improved thermal penetration depth will more than offset the increased conduction loss. Furthermore, if reduction of the conduction loss becomes necessary, this could be accomplished by designing small standoffs during the etching process to increase the thermal resistance of the stack.

Friction Factor

Tests were conducted using a steady flow of helium gas to determine the inlet pressure required to force a given mass flow through the regenerator housing packed with different matrices. A schematic of the test setup is shown in Fig. 7. The pressure differential across the regenerator was measured for several values of mass flow. Using this information, the friction factor (f) was determined using Eq. (2):

$$f = \frac{2\Delta p * D_h}{\rho L U^2} \tag{2}$$

In this equation, Δp is the measured pressure differential, ρ is the density calculated using the ideal gas law at the average pressure ($p_{atm} + \Delta p/2$) and ambient temperature, L is the axial length of the regenerator, and U is the average bulk fluid velocity, which is determined using the measured steady state mass flow divided by the previously determined density and free flow area. D_h is the hydraulic diameter and is determined by Eq. (3):

$$D_h = \frac{4(\alpha V_R)}{S_h} \tag{3}$$

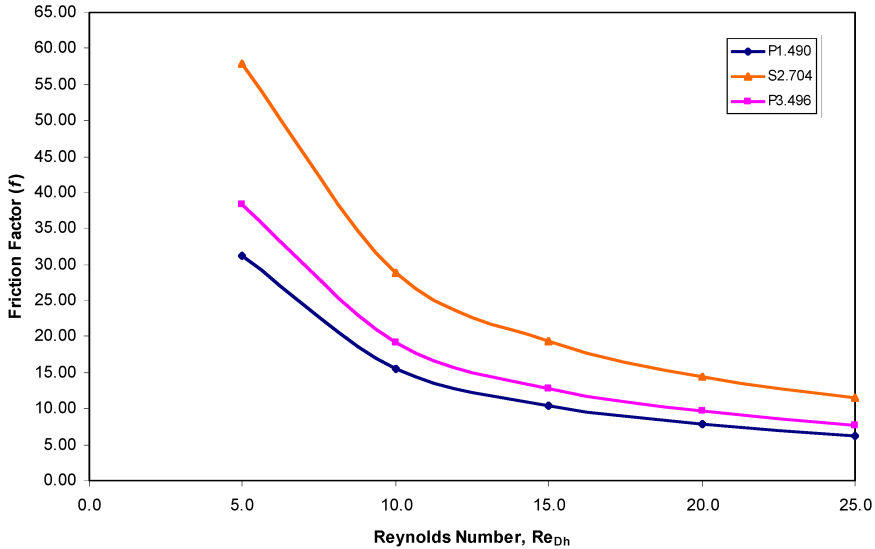
Here, V_R is the regenerator volume, α is the porosity, and S_h is the heat transfer surface area. The friction factor was then plotted as a function of Reynolds Number as determined from Eq. (4):

$$Re_{D_h} = \frac{\rho U D_h}{\mu} \tag{4}$$

The only variable in this equation not previously defined is the viscosity, μ . Friction factor is presented in Table 2, and these data are plotted vs. Reynolds Number in Fig. 8. P1.490 designates an etched disk matrix pinned to align the etched slots. P3.495 is the same etched disk regenerator, but the disks are randomly stacked, and the slots are not aligned. S2.704 is a 400 mesh screen matrix.

Table 2. Friction factor data for three different matrix configurations.

Mass Flow [g/s]	f			$f \cdot Re_{Dh}$		
	P1.490	S2.704	P3.496	P1.490	S2.704	P3.496
0.1	34.2	412.1	69.0	161.7	287.7	191.8
0.2	16.4	206.4	34.0	154.7	288.2	189.1
0.3	10.8	142.0	23.0	153.2	297.3	191.8
0.4	8.3	106.4	17.9	155.8	297.0	199.3
0.5	6.7	82.8	14.3	159.2	289.2	198.4
	Average			156.8	291.4	193.7

**Figure 8.** Friction factor data acquired from steady flow pressure drop measurements.

As expected, the product of friction factor and Reynolds Number is approximately constant. Although the maximum Reynolds Number attained in an operating cryocooler regenerator is likely higher than the maximum attained during steady flow testing, the fact that the product $f \cdot Re_{Dh}$ is a constant should remain. It should be noted that when the etched slots are not aligned, the surface area for heat transfer is increased while the porosity-regenerator volume product remains unchanged. The result is a decrease in the hydraulic diameter. This is because 50% of the top and bottom surface of the web is exposed to helium flow regardless of the angular orientation between webs of adjacent disks. As can be seen in Fig. 6, this results in a higher friction factor. However, it may offer advantages if performance is being limited more severely by the reduced heat transfer surface area of the etched disks.

REGENERATOR MODELING PROCEDURES

The use of REGEN3.2 to design a regenerator capable of producing refrigeration at 20K required that appropriate scaling parameters be determined to estimate actual heat transfer and friction characteristics of the etched disk matrix. The model inputs were first adjusted to accurately predict performance of a 400 mesh screen matrix operating in a pulse tube. It is assumed that friction factor and heat transfer correlations for screens that have successfully been employed in the design of cryocoolers for a long period of time are sufficiently accurate approximations. However, heat transfer and friction correlations for etched-disk matrices will likely require a scaling parameter to force agreement with the measured data. Before this can be accomplished, modeling procedures and the isothermal efficiency of the pulse tube expansion process need to be determined.

Screens

The modeling program REGEN3.2 is being used to evaluate the performance characteristics of the regenerator. The program requires certain operating characteristics of the cryocooler and dimensions of the matrix be known as input parameters. Wherever possible, these parameters were measured; otherwise, best estimates were used. The program requires that the amplitude and phase angle of the mass flow relative to the pressure at the cold end be known as well as the average pressure, warm and cold end gas temperatures, and operating frequency. It is assumed that a phase angle of -20 degrees is attainable with an optimized inertance tube. The amplitude of the pressure wave is measured at the inlet to the inertance tube and is assumed to be close to the pressure amplitude in the expansion volume. The water jacketed aftercooler is assumed to maintain a warm gas temperature of approximately 305 K. The cold gas temperature is proportional to the measured refrigeration temperature and applied heat load. This is due to the fact that a temperature difference between the gas and cold heat exchanger wall must exist to facilitate convective heat transfer. The cold heat exchanger consists of radial flow channels connecting the regenerator and pulse tube. The Nusselt number, defined in Eq. (5), can be determined from the flow channel geometry.²

$$Nu = \frac{hL}{k} \tag{5}$$

Here, h is the heat transfer coefficient, L is the channel length, and k is the helium conductivity. Using Newton’s law of cooling allows the gas temperature difference, ΔT to be determined from Eq. (6), where Q is the refrigeration power and A_w is the heat transfer surface area.

$$\Delta T = \frac{QL}{Nu * kA_w} \tag{6}$$

Now the cold gas temperature can be estimated by reducing the measured refrigeration temperature at the cold plate at an applied heat load. Figure 9 shows the dependency of refrigeration capacity on cold gas temperature based on REGEN3.2 output. The calculated ΔT at 77 K with a 5 watt heat load was approximately 4 K. The mass flow at the cold end is determined by varying its amplitude until the PV power at the warm end using REGEN3.2 matches the measured value obtained during testing. The pulse tube operates at a constant frequency of 60 Hz. The required regenerator matrix input is regenerator area, length, porosity, material, hydraulic diameter, and geometry (i.e. screens, parallel plates, etc.). All of these quantities are based on measured values.

The refrigeration capacity of the cryocooler is calculated based on an isothermal expansion process in REGEN3.2. It was assumed that this is why the modeling program predicted a performance of 11.1 watts using 400-mesh screens compared with a measured value of approximately 5.8 watts. If the isothermal efficiency is reduced to 74%, the predicted refrigeration correlates well with measured values.

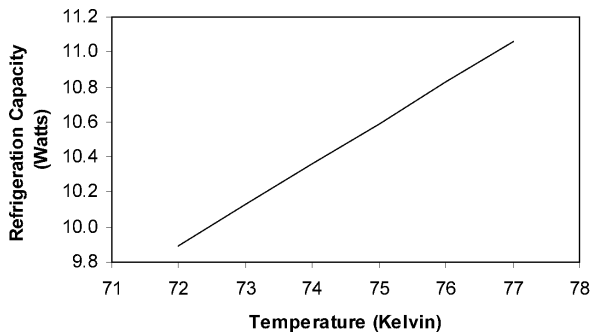


Figure 9. Predicted variation of refrigeration capacity on cold gas temperature using REGEN3.2.

Etched disks

The etched disk regenerator was installed in the pulse tube cryocooler, and the cold end temperature reached a minimum of 98 K. The pressure ratio and mass flow will be adjusted along with the friction factor scaling parameter in order to produce the measured compressor PV power. A heat transfer scaling parameter will then be determined to force the program output to agree with the measured data. This is the scaling parameter that will be used when modifying the regenerator dimensions in order to determine the optimal geometry for etched disks needed to attain the design goal of 2 watts of refrigeration at 20 K. An equation will also be input to the program to estimate the increased heat capacity of Holmium below temperatures of 100 K.

ACKNOWLEDGMENT

This program is being funded by the National Aeronautics and Space Administration (NASA) through the Small Business Innovative Research Program.

REFERENCES

1. Radebaugh, R., and B. Louie, "A Simple, First Step to the Optimization of Regenerator Geometry," Third Cryocooler Conference, Boulder, CO, (1984).
2. White, F.M., *Viscous Fluid Flow*, McGraw-Hill, NY (1991).